

CHAPTER 3

Prediction and Measurement of Specific Impulse

JEAN-PAUL BAC

1. Introduction

In the previous two chapters the importance of specific impulse has been noted several times.

All new propellant formulation research, or preliminary design analysis of a solid rocket motor, assumes knowledge of a theoretical value for specific impulse whence it is possible to start the analysis and give a direction to the research.

In most cases, calculations of the theoretical value of the specific impulse are performed with the assistance of thermochemical computations. The principal algorithms which are used throughout the world come from a computer program developed at the Lewis Research Center of NASA [1].

This chapter is a succinct description of the process, to allow the reader to understand the sequencing of the main phases of calculations to create a model for the gas and condensed phase* mixture from the combustion chamber to the exit plane of the nozzle.

Such models lead to solution of a system of equations with partial derivatives as a function of time and spatial coordinates [1-3]. The calculations themselves require access to the JANNAF thermochemical tables. These tables were first issued in 1971 and are periodically updated [4].

The purpose of Section 2 is to present and discuss a very simplified model, based solely on thermodynamics. It is specifically designed to provide an approximate value for the main operating parameters of a rocket motor without having to solve a differential equations system.

The application of the model to obtain predictions, followed by the experimental method for the measurement of the specific impulse, is dealt

* Condensed phase = combustion products in solid or liquid state.

within Sections 3 and 4. The chapter ends with a discussion of special application to performance predictions for solid fuels for ramjets.

N.B. The thermodynamics values used in this chapter are written as follows:

- Italic capitals: characteristic values of the overall system.
- Script capitals: molar values.
- Italic lower case: values per unit of mass.

2. Physical Model

2.1. DESCRIPTION OF THE MODEL

Physical phenomena associated with rocket motor combustion and flow processes are complex; it is therefore necessary to use a model based on an ideal motor, operating under a number of simplifying assumptions, to perform the required calculations.

More specifically, the combustion in the chamber is assumed to be adiabatic, at constant pressure, and yielding to a mixture of ideal gases and condensed phase products that are incompressible with a negligible molar volume in comparison with the gases. In addition, this mixture is in thermodynamic equilibrium at zero velocity. The combustion is followed, in the nozzle, by an isentropic flow, steady and quasi-one-dimensional, during which the condensed phases remain in thermal and kinematic equilibrium with the gas.

The assumption of steady flow allows us to work on the basis of per unit mass values.

The thermodynamic condition of adiabatic equilibrium maximizes entropy while observing the law of conservation of matter. Because we are assuming a transformation under constant pressure and at zero velocity, conservation of enthalpy (h) also occurs. With constant pressure and enthalpy, maximizing entropy is equivalent to minimizing Gibbs free energy:

$$g = h - Ts.$$

The use of the various assumptions given above allows us to progressively build a system of equations which, when solved, provides the values of the major operating characteristics of an ideal rocket motor.

2.1.1. Conservation of mass

For each of the elements of the chemical species included, we can write:

$$b_i = \sum_{j=1}^{ns} a_{ij} n_j = b_i^0; \quad i = 1, \ell \quad (1)$$

where:

- ℓ = number of elements;
- ns = number of species;
- a_{ij} = number of atoms of element i in a species of type j (a species is a given chemical compound or element in a given physical phase);
- n_j = number of moles of these species in the mixture;
- b_i = number of atom-grammes of element i in the propellant grain.

2.1.2. Minimizing free energy

Using the Lagrange multipliers λ_i linked to these equations, this condition is written as:

$$\mu = (\partial g / \partial n_i) T, p, \{n_k; k \neq j\} = \sum_{i=1}^{\ell} \lambda_i a_{ij}; \quad j = 1, ns \quad (2)$$

where g is the free energy per kilogram of mixture, T the gas temperature, and p the pressure.

Writing gases from 1 to m and the condensed products from $(m+1)$ to ns ($= m + nc$), (where nc stands for the number of condensed species), we have:

$$\mu_j = \mu_j^0(T) + RT \ln n_j/n + RT \ln p/p^0; \quad j = 1, m \quad (2a)$$

$$\mu_j = \mu_j^0(T); \quad j = m+1, ns \quad (2b)$$

- μ_j is the free molar energy (or thermodynamic potential) of the pure j species, in the same physical state (solid, liquid or gaseous) as the phase where this species is found in the mixture, under standard atmospheric pressure p^0 and at the temperature of the mixture.

- n is the total number of moles in the gaseous phase:

$$n = \sum_{j=1}^m n_j \quad (3)$$

2.1.3. Enthalpy conservation

With \mathcal{H}_j as the molar enthalpy of species j and h the enthalpy per unit of mass of the propellant grain, we can write:

$$h = \sum_{j=1}^{ns} n_j \mathcal{H}_j(T) = h_0 \quad (4)$$

When p is known, we have a system of $(1 + ns + 2)$ eqns (1)-(4) with $(1 + ns + 2)$ unknown $[(\lambda_i), (n_j), n$ and $T]$.

This system is perfectly defined and can therefore be solved, and it is possible to calculate the entropy at equilibrium s .

2.1.4. Isentropic expansion

This assumption enables us to write:

$$s = \sum_{j=1}^m n_j \mathcal{S}_j^\circ(T) - R \sum_{j=1}^m n_j \ln n_j / n p^\circ = s_0 \quad (5)$$

- \mathcal{S}_j° the molar entropy of the pure species j , under standard atmospheric pressure p° , in the same physical state (solid, liquid or gaseous) as the phase where this species is found in the mixture, and at the temperature of the mixture;
- s_0 the entropy per unit of mass in the chamber.

Two types of calculations are performed:

- expansion at thermodynamic equilibrium;
- expansion in frozen composition

In both cases the system is determined by the knowledge of the pressure.

In the first case we have a system of $(1 + ns + 2)$ eqns [(1), (2), (3) and (5)] with $(1 + ns + 2)$ unknowns [(λ_j) , (n_j) , n and T], and in the second case one eqn (5) with one unknown T .

Consequently, we can calculate the mass per unit volume $\rho = p/nRT$, the enthalpy $h(T)$ per unit of mass, the coefficient of isentropic expansion $\gamma_s = (\partial \ln p / \partial \ln \rho)$, and the velocity of sound:

$$a(T, p) = \sqrt{\gamma_s nRT}$$

2.1.5. Steady-state expansion

With v , the combustion gas velocity, we can write:

$$h + \frac{v^2}{2} = h_0 \quad (6)$$

i.e.

$$v = \sqrt{2(h_0 - h)} \quad (6')$$

The sonic throat of the flow is defined by:

$$v = a \quad (7)$$

The throat pressure ratio is determined through iterations on the pressure calculation, starting with the combustion pressure (p_0).

2.1.6. Assumption of a one-dimensional linear flow in the exit cone

Indices x , s and t designate, respectively, any cross-section of the divergent part of the nozzle, the section in the exit plane of the nozzle, and the section at

the throat of the nozzle. The equation of the conservation of mass is written as:

$$\rho_s A_s v_s = \rho_t A_t v_t = \rho_0 A_0 v_0 \quad (8)$$

It is therefore possible to:

- either select a value for the ratio of sections $\varepsilon = A_s/A_t$ and calculate the exit conditions with iterations on the pressure;
- or select the exit pressure and calculate the other parameters, including the sections ratio.

Using the various assumptions above, it is possible to write the equations required for the thermodynamic calculations and hence obtain the data that characterize the flow of gases and condensed products.

These data are then used to calculate the parameters characteristic of the operating point of the perfect motor. For example, the value of v_s obtained from eqn (6') can be used for either of the following purposes:

- either the calculation of standard adjusted expansion with $p_0 = 7 \text{ MPa}$ and $p_s = p^* = p^\circ = 0.1 \text{ MPa}$, obtaining the standard specific impulse $I_s = v_s/g_0$;
- or the calculation of expansion in a vacuum at given ε and obtaining the specific impulse in a vacuum $I_{vac} = v_s/g_0 + p_s/\rho_s v_s g_0$.

If the values of A_s and A_t are also selected, in addition to the values of ε , we can calculate:

- the mass flow rate: $\dot{m} = v_s A_s \rho_s$
- the thrust: $F = \dot{m} v_s + (p_s - p_a) A_s$

The following are also calculated:

- The flow rate, or discharge coefficient:

$$C_D = \frac{\dot{m}}{\rho_0 A_t} = \frac{\rho_t v_t}{\rho_0}$$

- The characteristic velocity:

$$C^* = 1/C_D = \frac{P_0 A_t}{\dot{m}} = \frac{P_0}{\rho_t v_t}$$

- The thrust coefficient:

$$C_F = \frac{F}{\rho_0 A_t} = I_s C_D g_0$$

2.2. LIMITATIONS OF THE MODEL

2.2.1. General assumptions

The thermodynamic model used is concerned only with the area related to the propellant gas volume, whose characteristics are calculated in the combustion chamber and then during the expansion in the nozzle.

We have to apply the laws of macroscopic physics and chemistry: the conservation of mass, the principles of dynamics, the first law of thermodynamics, the law of thermodynamic state, and laws of chemical kinetics and physical kinetics of changes of state. These laws were written for closed systems with the presence of physical equilibrium, which is not the case with the open system to which we are applying them. This is tantamount to considering the gas as closed subassemblies under physical equilibrium, i.e. considering the flow to be much more "orderly" than it really is. The gain in entropy is thereby underestimated; consequently, the mechanical efficiency — i.e. the impulse — is overestimated.

The amount of this overestimation cannot be predicted. This oversimplification must be done, unless all interactions between the atoms were to be written and integrated within the whole motor.

It is assumed that the gas is neither viscous nor heat-conductive (and consequently, that the phenomenon is adiabatic), and that the condensed products stay in thermal and kinematic equilibrium with the gas.

This assumption is not absolutely essential to do the calculation, but it simplifies it greatly. It also results in an overestimation of the impulse, which is particularly significant when the propellant produces condensed products. There is, indeed, a thermal and kinematic disequilibrium between the condensed products and gas, the latter being both more rapid and less hot than the condensed products.

The adiabaticity assumption, a corollary of the non-conductivity of the gas, also leads to an overestimation of the thrust. This is particularly true when the motor is small and not very well insulated.

In spite of the reservations listed above, this set of assumptions allows us to write eqns (1) and:

- The global equation for the conservation of mass:

$$d\rho/dt + \rho \operatorname{div} \vec{v} = 0 \quad (9)$$

- The equation for the fundamental law of dynamics:

$$\vec{\rho\gamma} + \operatorname{grad} p = 0 \quad (10)$$

- The equation for first law of thermodynamics:

$$\rho \frac{d\left(u + \frac{v^2}{2}\right)}{dt} + \operatorname{div} p \cdot \vec{v} = 0 \quad (11)$$

u = the internal energy per unit of mass of the combustion product.

- The equation of state:

$$\rho = \rho(T, p, \{n_j\}; j = 1, ns) \quad (12)$$

- The kinetic laws:

$$\frac{dn_j}{dt} = \dot{n}_j(T, p, \{n_k\}; k \neq j); j \neq j_i \quad (13)$$

The number of eqns (13) is equal to the number of species, less the number of elements in their standard state, i.e., $(ns - 1)$.

Equation (10) is a vectorial equation that corresponds to three differential equations. We therefore have a system of $(6 + ns)$ differential equations with $(6 + ns)$ unknowns $v_x, v_y, v_z, T, p, \rho$ and $\{n_j\}$.

2.2.2. Assumption related to the combustion chamber

First it is assumed that the gas velocity, and consequently the pressure gradient, is negligible in the combustion chamber. This approximation is reasonably well justified, particularly in the case of a large motor operating at low maximum pressure.

It is further assumed that gases in the entry plane of the nozzle are in thermodynamic equilibrium. This assumption is consistent with the previous one. It is also fairly well justified, particularly in the case of a large, well-insulated motor.

These are the two assumptions used to calculate initially an equilibrium at constant pressure at zero velocity in the combustion chamber.

2.2.3. Assumption related to the gas expansion

The flow is considered to be isentropic. This is not a good assumption since an actual flow is by nature irreversible, and therefore non-isentropic, if it is adiabatic. This particular assumption contributes greatly to an overestimation of the impulse. As for solving the equations, it enables the creation of a relation independent of time and spatial coordinates, between the number of moles, the temperature and the pressure. But it is of no interest if it is not complemented by an assumption which enables us to by-pass equations of

chemical kinetics (13). It explains (but does not justify) the decision to perform two calculations, one in thermodynamic equilibrium and the other in which the composition remains unchanged. *All other assumptions being equal*, the truth lies somewhere in between, closer to equilibrium in the convergent part of the nozzle and closer to frozen composition in the divergent part of the nozzle. Expansion in thermodynamic equilibrium overestimates the impulse, while expansion assuming frozen composition underestimates it.

Using these two complementary assumptions (isentropic flow and thermodynamic equilibrium, or frozen composition), the choice of a pressure determines the temperature and the composition of the mixture.

We then assume a steady-state flow. This assumption is justified by the fact that we are generally looking to obtain an operation which stays quasi-steady during the major portion of its duration. This assumption contributes to an overestimation of the impulse inasmuch as, all other assumptions being otherwise identical, steady-state specific impulse is always greater than specific impulse which is calculated including the pressurization and burnout phases.

Under this steady-state flow assumption (9), the equation reads:

$$\operatorname{div} \rho \cdot \vec{v} = 0 \quad (14)$$

Combining eqns (14) and (11) gives:

$$\frac{d\left(u + \frac{v^2}{2} + \frac{p}{\rho}\right)}{dt} = \frac{d\left(h + \frac{v^2}{2}\right)}{dt} = 0 \quad (15)$$

The quantity $(h + v^2/2)$ is therefore constant along a streamline. Since all flow lines start from the entry section of the nozzle, we can write:

$$h + \frac{v^2}{2} = h_0 \quad (16)$$

2.2.3.1. Analysis of the conditions at the throat of the nozzle

With a steady flow the location of the sonic throat of the flow is stable. It is located at the actual geometric throat of the nozzle.

Equation (14) can then be replaced with

$$v = a$$

to determine, iteratively, the pressure at the throat.

The transformation of propellant into gas is accompanied by an increase in volume. Combustion produces a gas with a velocity v_c , such as:

$$v_c = \frac{dV}{S dt} = \frac{1}{S} \frac{dV}{dm dt} = \frac{1}{S} \left(\frac{1}{\rho_c} - \frac{1}{\rho_p} \right) \dot{m}$$

where:

ρ_c = mass per unit of volume of the gases inside the combustion chamber;

ρ_p = mass per unit of volume of the propellant grain;

v = volume of the propellant grain;

s = burning area of the propellant grain.

Our steady combustion assumption requires that we neglect $1/\rho_p$ before $1/\rho_c$ and write:

$$\dot{m} = \rho_p S v_r = \rho_c S v_c = \rho_c A_t v_t$$

where v_r is the burning rate of propellant grain for a pressure p_0 in the combustion chamber.

If velocity v_r is known, the burning area to throat area ratio $K = S/A_t$ can be determined, and by iterations on the pressure of the chamber, the burning rate at which a steady operation should occur can also be determined.

2.2.3.2. Analysis of the conditions in the divergent part of the nozzle

Using previous assumptions (adiabatic, isentropic and steady expansion, in equilibrium or with frozen composition), the knowledge of the pressure at one point determines the temperature, the composition of the mixture, and the velocity of the flow at that point.

To simplify calculations an unrealistic approximation is made, for modeling this segment of the nozzle: the pressure is assumed uniform over any nozzle cross-section, and, consequently, that the velocity is everywhere parallel to the axis.

Therefore, the equation for the conservation of matter is written as

$$\rho_c A_t v_c = \rho_x A_x v_x = \rho_l A_l v_l$$

Because of that, the following results are obtained, in a cross-section:

- a pressure and mass per unit of volume which are constant for the entire cross-section rather than increasing from the periphery to the center;
- a velocity which is constant for the entire section instead of decreasing from the center to the periphery (v instead of $v \cos \alpha$, α being the half-angle at the apex of the divergent part).

As a result, this approximation:

- leads to an overestimation (all things being otherwise equal) of the ratio of cross-sectional areas necessary to obtain fixed expansion;
- contributes to the overestimation of the impulse by an amount that cannot be exactly determined, although it is known to be of the order of $(1 - \cos \alpha)$, and therefore of about 1%.

Finally, in order to analyze what occurs in the exit section of the diverging part of the nozzle, it is necessary to research the interaction of the jet with the merging air stream. This problem is far more complex, and resolving it is completely out of the question. The assumptions necessary to bring its complexity down to the level of the preceding assumptions would completely change its characteristics. We therefore limit ourselves to:

- Assuming that $p_s = p_a$ for an expansion at a given ambient pressure, and then calculating the corresponding cross-sectional area ratio. However, p_s is necessarily greater than p_a because the velocity can be different from zero in a given direction only if the pressure diminishes along the corresponding streamline. But this difference is very small, because the ejected gas molecules have an infinite expansion volume, so that they are in an infinitesimal minority compared to the merging air stream and the velocities resulting from intermolecular collisions rapidly become random. This simplification does contribute to an overestimation of the impulse, although to a much less important degree than with the preceding assumptions.
- Calculating p_s regardless of p_a , for a given expansion ratio.

If p_s has been determined to be much greater or smaller than p_a , the impulse calculated will have no significance, because there probably will be no steady operation with such a pressure mismatch.

If p_s is determined to be a little less than p_a , then the entire set of assumptions is self-consistent, and provides a specific impulse with a good indicative value.

2.2.4. Conclusion

In conclusion, the specific impulse calculated using this model is always overestimated. The smaller the rocket motor, the higher mass fraction of condensed phase material elements in the combustion gases and therefore the higher this overestimation. With a propellant producing no condensed phase products the overestimation will be highest if the combustion gas viscosity and thermal conductivity are higher. (For a propellant grain producing condensed products, there are combinations of viscosity and conductivity for which the overestimation is minimal, all other assumptions being equal.) It is necessary to have a value of this overestimation to determine the average specific impulse of rocket motor. A range of values is found in Chapter I.

The specific impulse determined in this manner provides mainly a comparative value. Even then, great caution is required since, disregarding the size factor, the deviations between the calculated and the actual specific impulses depend on the intrinsic characteristics of the propellant, i.e.

- its physical structure, which plays a major role in the degradation mechanism;
- its basic composition and the molecular structure of the chemical components, which determines its enthalpy, its free energy, its reaction mechanism in the gaseous phase, and the ballistic characteristics (isentropic ratio, viscosity and thermal conductivity) of the combustion gases.

Since each one of these characteristics plays a special role in the deviations between the actual specific impulse and its calculated value, there is no reason to believe that ratio " I_s predicted versus I_s actual" will be identical for all propellants. It is more accurate to state that this model offers the possibility of a valid classification of the propellant within a particular family, and also for propellants with the same molar ratio of condensed products. But caution is advised when comparing two different propellant families. Since the deviation between the actual specific impulse and predicted value is of the order of 10% for any one propellant, a calculated difference of 4-5% between families of propellant is not necessarily meaningful.

3. Predictions

Specific impulse predictions are commonly used in two main areas:

- new propellant formulation research;
- determination of the theoretical performance of a rocket motor.

3.1. NEW FORMULATION RESEARCH

Technical requirements such as guidance and low signature, related to the mission of the missile (particularly in the tactical area), affect the selection of the propellant. In addition to highest performance, the designer must also look for formulations with combustion gases that provide, for example:

- No absorption of electromagnetic waves required for missile guidance. This absorption is caused by the ionization of the gases, particularly alkaline or alkaline-earth.
- No absorption in infrared — another factor in guidance — which supposes aluminum contents lower than 0.5%.
- No absorption in the visible range, to avoid detection of the missile, requiring a plume containing no condensed elements and without any of the HCl-type gases, i.e. gases that can condense when combined with molecules of the atmosphere (H_2O in this case).

The calculated results include the chemical compositions of the plume, allowing its classification according to the established characteristics for operational requirements.

In addition, when identifying the optimum composition from a family of

propellants, a parametric analysis is performed using the three major components (for example, the binder, ammonium perchlorate and aluminum). A ternary diagram is drawn (Fig. 1). Studying the curves I_t , T_c , or $\rho \cdot I_t = \text{constant}$ allows the selection of the highest performing propellant composition. Although a large number of complete calculations are required for these diagrams — approximately 30 for each propellant family — they are very frequently used. They afford substantial savings in cost and research time by limiting the number of experimental tests that would have to be performed for such a selection.

3.2. DETERMINATION OF THE THEORETICAL PERFORMANCE OF A ROCKET MOTOR

Based on the technical requirements of a rocket motor, total impulse: IFT , combustion duration, dimension and on the theoretical specific impulse selected, the calculations related to the ballistics (Chapters 1 and 2) also allow the identification of an average operating point (c , P_0 , P_2).

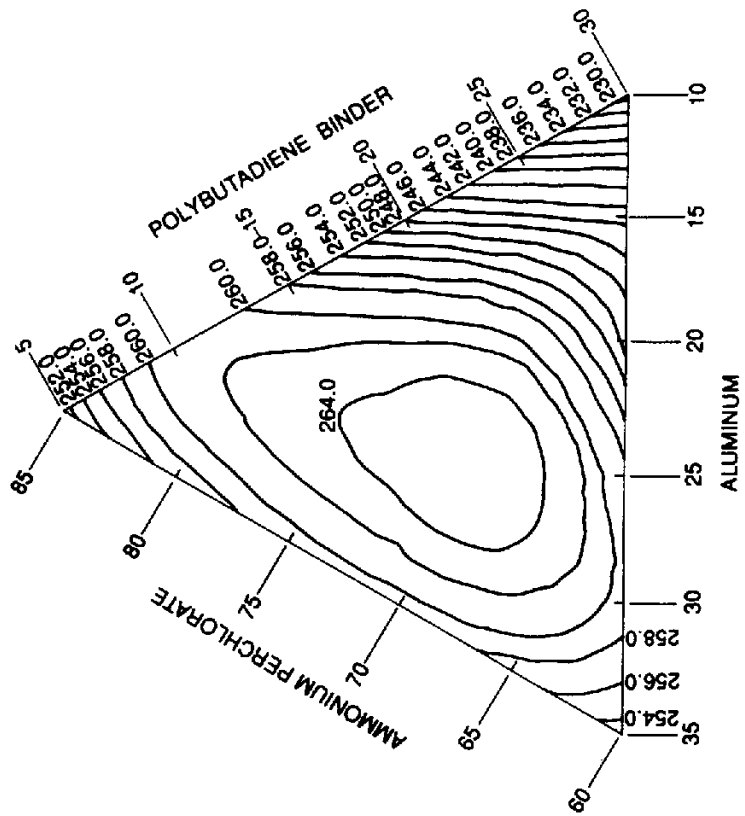


FIG. 3.1. Theoretical specific impulse diagrams (seconds).

The previously defined thermochemical computations are typically programmed for computer solutions. Using results from such a computation, the preliminary analysis designer is able to calculate the theoretical performances of the rocket motor. In addition to the values of the specific impulse (fixed nozzle expansion and expansion to vacuum), he can also obtain the exact composition of the plume as well as the thermodynamic values (C_p , γ , μ , M , H , S) which characterize the system.

These values will be used as entry data to calculate the flow in the combustion chamber (Chapter 4), or the loss of performance in the nozzles (Chapter 1).

The thermochemical computations are also used to predict the theoretical performance of more complex chemical systems, such as:

- rocket motors using end-burning propellant grains for which the gases from the erosion of the thermal insulation and inhibitors must be taken into account with the combustion gases of the propellant grain [6];
- ramjets using solid fuels for which the mixing of combustion gases with air needs to be calculated (Section 5 of this chapter).

4. Measurement of the Specific Impulse

4.1. INTRODUCTION

Whether determining the value of the specific impulse of a propellant or of any rocket motor, this prediction requires:

- the use of test facilities designed for the purpose (firing stand);
- the acquisition of all data (pressure, thrust, time, mass, etc.) with a maximum of precision;
- a very exact description of the methods used to interpret the results.

The following section describes the equipment necessary to perform the tests, as well as the various operations performed, using as an example the prediction of the standard specific impulse of a propellant.

4.2. THE THRUST STAND

The thrust stand must be capable of withstanding and accurately monitoring the full thrust developed by a rocket motor. There are various types of firing benches, including:

- the blade bed,
- firing beds with sliding plates,
- vertical benches,
- pendulum gun,
- spinning benches.

The blade bed is most widely used to determine the characteristics of a propellant by firing standard configuration propellant grains. It is shown in Fig. 2; the rocket motor is attached to a very rigid frame suspended from rigid supports with a set of flexible blades. The role of the blades is strictly limited to that of a mechanical linkage, having no impact whatsoever on the thrust measurement. They must not be too flexible, to avoid parasite vibrations resulting from ignition of the rocket motor.

The thrust of the rocket motor is transmitted to a load cell.

The continuity of the load cell is completed by a pre-load screw which is attached to a block of solid concrete that absorbs the thrust of the motor.

The bench construction must be done carefully to ensure a perfect alignment between the thrust axis of the rocket motor and the axis of the cell.

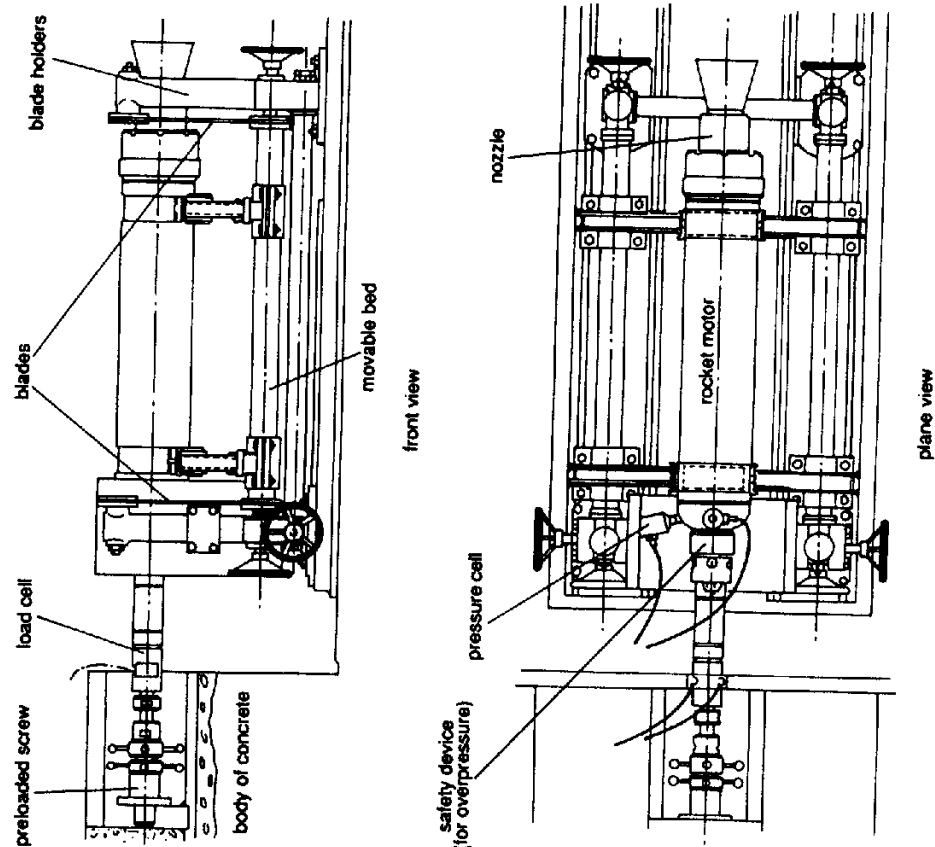


FIG. 3.2. Test bench.

4.3. THE STANDARD MOTOR AND HEAVY WALL MOTOR

This is the test motor configuration used to determine the average standard specific impulse (I_{sp}). The description given in this section is related to the French standard. This equipment is specially designed for repetitive tests necessary when the measurements taken are for the control of industrial production, or for development analysis. For the latter, the metal parts are over-sized, and those parts that have not been heavily exposed to combustion gases (front end and the cylinder) can be reused with a limited amount of maintenance work. On the other hand, because of the importance of their definition for the precision of the measurements, certain subassemblies (nozzle throat, exit cone) are systematically replaced.

The complete assembly includes three major parts:

- (1) An end base, equipped with a rupture disc to limit the pressure in case of a problem during combustion. The pressure and thrust cells are attached to the base. Thermal insulation is placed in the inside of the motor.
- (2) The propellant grain which is contained in a cylinder for cartridge landing (this may also be insulated).
- (3) A cylindrical part, where the free-standing propellant grain is placed. This may also be thermally insulated.
- (4) A rear assembly, made also of three parts: a convergent section, or nozzle, a nozzle throat, and a divergent section (Fig. 3).

Concerning the convergent section of the nozzle:

- it is made of a heat-resistant material (composite or graphite material);
- the half-angle of the convergent section is 45° — the diameter at entry is equivalent to the diameter of the free-standing propellant grain;

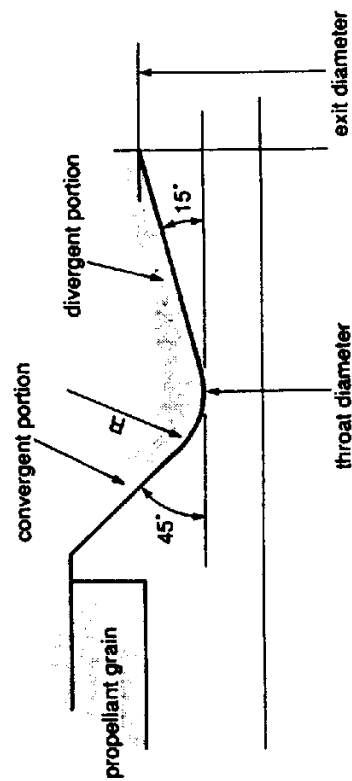


FIG. 3.3. Rear assembly.

- no discontinuity is permitted in the convergent section of the nozzle, including at the junction with the throat of the nozzle;
- the surface must be as smooth as possible.

Concerning the throat of the nozzle:

- it is usually made of graphite;
- the radius R of the junction where the convergent and divergent portions meet is such that $R > \varnothing$ throat;
- the diameter of the throat is a function of the size of the free-standing grain, of the composition of the propellant, and of the desired pressure.

Concerning the divergent section:

- it is very often made of composite material;
- the half-angle of the divergent part is 15° ;
- the exit diameter is calculated as a function of the desired expansion.

4.4. THE PRESSURE TRANSDUCERS

- Two types of pressure transducers are used on the motors.
- Piezoelectric sensors with a broad frequency response to allow detection of rapidly changing combustion phenomena.
- Strain gauges to provide very precise measurements of the steady-state pressure curve.

4.5. THE PROPELLANT GRAIN

The selection of the propellant grain configuration is based on the following criteria:

- The burning area should have little dependence on the web burned so that the pressure as a function of time resembles a step function (instant rise, constant pressure plateau, instant pressure drop) as much as possible.
- The evolution of the grain burning surface should be as predictable as possible, which requires:
 - (a) a constant burning rate along the central port, devoid of any interfering phenomena such as erosive burning, or combustion instabilities (Chapter 4), and
 - (b) a very precise knowledge of all configuration characteristics, in particular the thickness of the web and the mass of the propellant grain.
- Fabrication should be simple and reproducible to reduce production costs.
- The mass of propellant should offer a good compromise between a value sufficient to limit errors related to measurement (weight, dimensions, etc.) and a value that respects the previous criterion.

A large number of types of propellant grains fulfilling these criteria are in use throughout the world. The more detailed description that follows is limited to two of the propellant grains often mentioned in this book.

4.5.1. The star-shaped central port propellant grain

This propellant grain, called MIMOSA as used in France, has a star-shaped central port with 10 segments. Its outer diameter is 203 mm; its weight is approximately 45 kg for 1 m of length. It has been used for a long time as a control propellant grain for the ballistic properties of composite propellants.

The neutrality of the burning grain surface evolution,

$$\frac{S_{\max} - S_{\min}}{S_{\text{average}}}$$

as a function of web burned, is very good.

The star shape, however, has the drawback of generating a burning surface area evolution which, as it evolves into the final phase (starting at the moment when the burning area is bordering the case), causes a pressure drop with a small combustion tail-off.

For research on new propellants the size of each sample propellant grain is kept small. This minimizes cost and enables evaluation of a large number of compositions. Another propellant grain called CAMPANULE may be used. Its weight is much lower (2.5 kg), with a 90 mm diameter and 300 mm length. It has a star-shaped central port, 10 segments, and provides initial data on the levels of specific impulse. Different companies or organizations use cylindrical smaller grains.

4.5.2. Perforated grain [7]

This is a propellant grain with a circular central port with flat, uninhibited end surfaces. This type of propellant grain, used in the United States, is known as the BATES (Ballistic Test Evaluation System). The burning area versus web burned is very constant, with no combustion tail-off: the pressure decrease at burnout is only controlled by the venting of the combustion chamber.

This propellant grain is available in several different sizes, as shown in Table 1. The 7-inch and 12-inch sizes are used in France to determine the characteristics of energetic binder compositions (Chapter 2) because of the very good tail-off curve. This is important for these formulations with high pressure exponent at low pressures which can lead to unburned residual propellant with other initial surfaces.

TABLE 1 Main characteristics of the various BATES propellant grains

Outside diameter (inches)	Length (inches)	Approximation propellant mass (kg)
7	12	6.5
12	20	35
28	60	380

4.6. MEANS OF MEASUREMENT

The measurement system must faithfully record the strain/stress signals given by transducers during the motor firing. The analog processing of the signal is not very precise, so a digital processing is usually preferred. A classic measurement system is shown in Fig. 4.1.

4.7. DETERMINING THE PARAMETERS OF A FIRING TEST

(N.B.: The exact definition of the parameters, as well as the equations used, are found in Chapter 1.)

This section involves the calculation, for a given propellant grain composition and type, of the three types of parameters discussed below.

4.7.1. Operating pressure of the firing test

The ideal, of course, is to reproduce standard operating conditions (expansion ratio 7/0.1, Chapter 1), which alone legitimize comparisons of

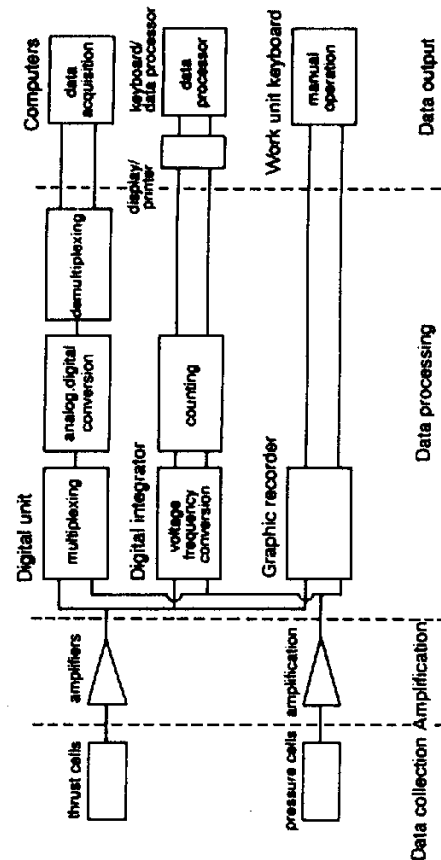


FIG. 3.4. Measurement system.

performance between various propellant grains. Consequently, the average value of pressure obtained during the firing test should be 7 MPa.

This value is representative of the operating range of most of the composite propellants (approximately 3-11 MPa), and will therefore be selected for the firing test parameters used in MIMOSA and BATES configurations.

Some double-base propellants differ, and have an operating range between approximately 15 and 30 MPa. They require a pressure curve corresponding to the plateau of their burning rate versus pressure curve (Chapter 9). These test conditions necessitate correction of the measurement data to obtain a final value that corresponds to the standard conditions.

4.7.2. Dimensions of the nozzle throat and of the exit plane

The diameter of the throat of the nozzle is calculated as follows:

$$C_D \cdot p_o \cdot A_t = \rho \cdot S \cdot v$$

where:

C_D = propellant discharge coefficient;

p_o = combustion chamber pressure;

A_t = area of the throat,

ρ = mass per unit of volume of the propellant grain;

S = burning area of the propellant grain;

v = burning rate of the propellant grain at pressure p_o .

The diameter of the divergent part of the nozzle (exit plane) is calculated as follows: using the throat diameter, and the section ratio $\varepsilon = A_e/A_t$ (ratio of the area of nozzle exit plane versus the area of the throat), we can determine the diameter of the exit plane. This ratio is a function of pressures p_o and p_e ; it also varies according to the value of for the propellant gases (Chapter 1). The thermodynamics calculations done for the propellant yield a value such that the pressure in the divergent exit plane is equal to the ambient atmosphere pressure.

In the case of aluminized propellants, when the test firing occurs with a chamber pressure in the range of 7 MPa (expansion ratio of gases p_o/p_e is 70), that value is of the order 10.

4.7.3. Other parameters

To select the transducers and calibrate the measurement system, the following are also determined:

- firing time: t = web to be burned divided by average burning rate;
- expected thrust: $F = C_F p_o A_t$, where C_F is the thrust coefficient of the nozzle (approximately 1.5 for $p_o = 7$ MPa).

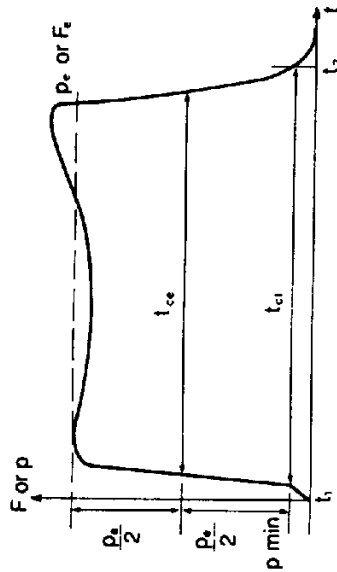


FIG. 3.5. Data analysis.

4.8. ANALYSIS OF THE RESULTING DATA

Figure 5 shows the definition of the parameters which need to be calculated to do a thorough analysis of the firing test, based on the measurements recorded (pressure or thrust versus time).

(1) Total combustion time, t_{ct}

Determination of p_{min} = atmospheric pressure + 1% of the maximum capacity of the pressure cell, gives t_1 and t_2 ; and the $t_{ct} = t_2 - t_1$

(2) Effective combustion time, t_{ce} and effective pressure, p_e

Based on the curve $p = f(t)$ obtained, these two parameters are calculated through a series of iterations. They are related through the equation:

$$p_e = \frac{\int_{t_1}^{t_2} p \cdot dt}{t_{ce}}$$

(3) Discharge coefficient, C_D

$$C_D = \frac{\text{Weight of propellant burned}}{\int_{t_1}^{t_2} p \cdot dt \cdot A_{tm}}$$

(4) Average area of the nozzle throat, A_{tm}

Because the variation as a function of time the throat diameter is not available, it is necessary to calculate the average area of the throat, based on mathematical averaging of the diameter before and after the firing.

(5) Mass of propellant burned

The propellant grains used must be carefully weighed during their manufacture.

Usually, the weight of the propellant grain is determined by deducting the weight of the inhibitor from the total weight of the manufactured free-

standing grain. It may, however, be necessary to weigh the inhibitor remaining after firing, particularly in the case of heavy ablation. If it is necessary to take into account the weight of inhibitor burned, its contribution is approximated as half of its weight in propellant.

(6) Average specific impulse, I_{sm}

The average specific impulse of the rocket motor tested is calculated using the equation

$$I_{sm} = \frac{\int_{t_1}^{t_2} F \cdot dt}{g_0 \times \text{weight of propellant discharged}}$$

(7) Standard specific impulse, I_{sm}

The average specific impulse corresponds to average operating conditions that may deviate slightly from the targeted theoretical values (pressure, expansion ratio).

Based on the values actually obtained during a test (ε , effective pressure, and atmospheric pressure), corrections are necessary to adjust the average specific impulse to the standard conditions.

To achieve this, we rely on the fact that, with the same propellant grain and similar operational conditions, the specific impulse of a rocket motor is proportional to C_F . This equation takes into account the data presented in Chapter 1 which demonstrated the following:

- the existence of the equation: $I_s = C_F / g_0 C_D$;
- the assumption of the independence of the mass flow rate coefficient C_D from the combustion chamber pressure during firings with a pressure close to standard conditions (7 MPa);
- The dependency of the thrust coefficient, C_F , on the operating pressure, the ambient pressure, and the cross-sectional area ratio (ε) of the nozzle.

The standard specific impulse is calculated from the equation:

$$I_{sm}^s = I_{sm} \cdot \frac{C_F \text{ (calculated for standard conditions)}}{C_F \text{ (calculated for the exact operating conditions)}}$$

The values obtained range from approximately 170 s to 255 s, according to the propellant families used.

REMARK: In some cases the operating point of a rocket motor may not be close to the standard conditions (7 MPa). In addition to the above correction it is necessary to include the deviation of the mass flow rate coefficient as a function of pressure. This deviation is calculated using and T_0 (Chapter 1). The equation is written:

$$I_{sm}^s = I_{sm} \cdot \frac{C_F \text{ (standard conditions)} \cdot C_D \text{ (operating point)}}{C_F \text{ (operating point)} \cdot C_D \text{ (standard conditions)}}$$

4.9. ACCURACY OF THE MEASUREMENTS

Many parameters play a role in the quality of the measurement of the specific impulse; they include:

- the accuracy of the pressure and thrust measurements (linked to the firing bench, the sensors, and the measurement system);
- the precision of the calculations done from the firing measurements taken;
- the accuracy of the evaluation of the weight of the propellant discharged (involving the inhibitor, deposits inside the combustion chamber and on the nozzle, and presence of unburned propellant in the inhibitor);
- insufficient knowledge of the variations of the throat area (and possibly of the nozzle exit area) during firing;
- a mismatched nozzle, due to pressure variations in the combustion chamber during firing;
- the presence of transitory phases (ignition phase and burnout phase).

As a result it is necessary to perform several firings under identical conditions so that the evaluation of the specific impulse of a propellant grain may be sufficiently precise (standard deviation $\sigma \approx 0.5-1$ s).

5. Solid Fuels for Air-breathing Systems

5.1. THE PHYSICAL PHENOMENA

Missiles powered by solid fuel ramjets or ducted rockets use oxygen-deficient propellants. The theory of operation has already been introduced in Chapter 1. These propellants, which are further described in more detail in Chapter 12, are greatly "under-oxidized", i.e. they contain just enough oxygen for complete gasification. These gases are formed in a primary chamber from which exhaust flow is generally restricted by a nozzle or valve. These gases flow into a secondary chamber, which is the real combustion chamber of the ramjet. Another system, which has already been flight-tested on a missile, did away with the intermediate nozzle by using propellants that burn at the pressure of the ramjet chamber. This type of configuration is called integrated gas generator or unchoked gas generator. For the two-chamber system the fuel-rich gases are injected into the secondary chamber where they mix with air coming through the air inlets located at the front of the missile. The major technical difficulty is the adjustment of the combustion gas flow rate to that of the air, to obtain a homogeneous and inflammable mixture under the actual conditions in the secondary chamber. The theoretical problem is therefore mostly one of dynamics of fluids and chemical kinetics. Thermodynamics helps to determine the upper value for the specific impulse that can be obtained at the exit of the secondary chamber.

5.2. ORGANIZATION OF THE CALCULATIONS

5.2.1. Determination of the properties of the propellant in the primary chamber

This first calculation (following the model described in Section 2 of this chapter) may be performed to obtain data for the thermodynamic parameters and the composition of the combustion gases.

In reality the global performance of the system is more useful. Consequently, the conditions in the secondary chamber are usually determined directly.

5.2.2. Determination of the propellant gas/air mixture in secondary chamber conditions

This calculation is based on the conservation assumption of the total dynamic enthalpy.

The calculation is the same as for a classic propellant grain. The only difference is that the enthalpy in this conservation equation ($h = h_o$) is no longer the propellant's enthalpy alone, but rather the sum of the propellant enthalpy and of the dynamic enthalpy of the air. We should note that the static enthalpy of the propellant has already been actually transformed into the combustion gas dynamic enthalpy, although it makes no difference for this global assessment.

The zero-velocity assumption in the combustion chamber results in even greater deviations than with classic rocket motors. In addition, since the entropy of the mixing of propellant gas and air is not taken into account, the total entropy gain in the chamber is higher than in a classic rocket motor, and the efficiency is overestimated.

However, in spite of this, the value obtained through calculations is very close to the values obtained through experiments.

5.2.3. Calculation of the expansion in the nozzle

This calculation is exactly the same as for a classic propellant grain, and the approximations call for just about the same remarks.

The zero-velocity assumption at the nozzle entrance is even more difficult to control. The additional amount of deviation is very small, however, because the assumption of sonic speed at the throat of the nozzle remains valid.

5.3. PERFORMING THE CALCULATION

5.3.1. Data entry

In standard calculations the data entry consists of the basic composition and the enthalpy of formation of the propellant. In the case of semi-propellant grains the proportions of the mixture, the propellant enthalpy, and the dynamic enthalpy of the air are also needed.

All quantities are expressed in mass, whereby:

f_s is the stoichiometric ratio of propellant combustion gases versus air,
 f is the ratio of propellant gases versus air of the mixture analyzed

$$\varphi = \frac{f}{f_s} \text{ is called the equivalence ratio.}$$

The proportions of the mixture may be determined with:

- either the air and propellant gas flow rates;
- or the equivalence ratio φ of the mixture.

The dynamic enthalpy of the air is calculated with the assistance of a second computer program based on the altitude and the Mach number. This same program is also useful for the calculation of static enthalpy at any temperature and altitude. As a rule the calculations are limited to sea-level altitude, which is a good representation for bench firing.

5.3.2. Results

With the propellant composition and the oxidizing potential, the values of the thermodynamic parameters in the secondary chamber, at the throat, and at the exit plane of the nozzle are obtained. For the various levels of φ selected we therefore obtain the global specific impulse of the mixture which can be expressed as:

- either the fuel-specific impulse (written: I_f);
- or the air-specific impulse (written: $I_{sa} = f \cdot I_s$)

The quantity $f \cdot I_s$ is also known as the air-specific thrust.

In a diagram " $I_s \cdot \rho - f \cdot I_s$ ", where ρ is the density of the propellant, the curve plotted for the various equivalence ratios characteristic of that particular propellant.

A comparison is generally made for the performance of the various solid fuels, for the standard conditions (20°C, Mach 2, sea level), and recording the values of $I_s \cdot \rho$ obtained for an identical value of $f \cdot I_s = 50$ s.

The analysis of this diagram provides the values of corresponding $f \cdot I_s$ for a set performance level (I_s). Because these values are directly tied to the air

consumption ($f \cdot I_s = I_{sa}$), the selection of a solid fuel is possible by taking into account the effect it will have on the size of the air inlets of the ramjet (which can be a more or less important factor of drag).

Based on the solid fuel formulation, the specific impulse I_s ranges from approximately 600 to 1300 s. (For comparison purposes only, the specific impulse I_s of the solid fuel alone, calculated under standard expansion conditions (7/0.1), is in the vicinity of 190 s.)

5.4. METHOD OF MEASUREMENT

Measuring the specific impulse of solid fuels for operating conditions of a ramjet is vastly more difficult to do than measuring standard specific impulse of a solid propellant. It requires testing installations which best simulate the overall operation of these motors, and in particular, access to an air-supply system.

Two types of test facilities are used, determined by the goal of the test performed [8].

The direct connect setup: the air inlets of the combustion chamber are directly connected to a hot air supply with a controlled flow rate. Because the pre-heating of the air enables the enthalpy to be brought to the dynamic level intended by simulation, this system offers a good representation of the operating conditions in the combustion chamber. Since it is relatively easy to set up, it is widely used. Unfortunately, because of its design it provides no information whatsoever on the aerodynamic phenomena related to air inlets. It is, however, the only system that allows easy thrust measurement during the performance of the test.

In the free stream setup, the supersonic flow of air necessary to properly simulate the actual supply of air to the air inlets is obtained by putting each of the air inlets within the exit plane of a nozzle. These nozzles are fed by a wind-tunnel system. In addition to the operating conditions in the combustion chamber, this setup has the advantage of providing data on the aerodynamic phenomena (shapes of the shock waves) linked to the actual geometry of the air inlets. It also allows observation of the transition phase between the burnout of the booster propellant grain and the ignition of the sustainer propellant grain when dealing with a ramjet with integral boosters inside the combustion chamber. This setup is much more complex than the previous one, and requires the installation of powerful wind tunnels.

Bibliography

1. GORDON, S. and McBRIDE, B. J., *Computer Program for Calculation of Complex Chemical Equilibrium Compositions, Rocket Performance, etc.* NASA Lewis, SP, 273, 1971.
2. ZELEZNIK, J. K. and GORDON, S. Calculation of Complex Equilibria. *Ind. Eng. Chem.*, 60(6), 27-57, 1968.

3. Kinetics and Thermodynamics in High Temperatures Gases. A conference held at Lewis Research Center, Cleveland, Ohio. NASA SP-239, March 1970.
4. STULL, D. R. and PROPHET, H., Project Directors. *JANNAF Thermochemical Tables*, 2nd edition. NSRDS-NRS 37. Catalog Number C13. 48:37. US Government Printing Office, Washington, DC, 1971.
5. CHASE, M. W. *et al.*, *JANNAF Thermochemical Tables*: 1974 supplement, *J. Phys. Chem. Ref. Data* 3, 311. 1974; 1975 supplement, *J. Phys. Chem. Ref. Data* 4, 1, 1975; 1978 supplement, *J. Phys. Chem. Ref. Data* 7, 793; 1978; 1982 supplement, *J. Phys. Chem. Ref. Data* 11, 3, 1982.
6. BANON, S. and ASTIER, J., The contribution of inert material to end burning propellant grain performances. AIAA 86.1421; AIAA/SAI/ASME; 22nd Joint Propulsion Conference. 1986.
7. COLLINS, R. G., The AFRPL Ballistic Test and Evaluation System (BATES Program). AFRPL Report No. TR-65-7. Air Force Rocket Propulsion Laboratory, Edwards, May 1965.
8. MAHONEY, J. J., Salient characteristics and development status of ramjets for guided missiles with emphasis on air launched tactical configurations. Naval weapons center technical memo, TM4452, October. 1981.